arXiv:1511.00497v1 [physics.plasm-ph] 2 Nov 2015

Current scaling and plasma heating in relativistic laser-solid interaction

T. Kluge,* M. Bussmann, L. G. Huang, and J. Metzkes
Helmholtz-Zentrum Dresden-Rossendorf, Germany

T. E. Cowan and U. Schramm
Helmholtz-Zentrum Dresden-Rossendorf, Germany and
TU Dresden, Germany

(Dated: Tuesday 3rd November, 2015)

Intense and energetic electron currents can be generated by ultra-intense lasers interacting with solid density targets. Especially for ultra-short laser pulses their temporal evolution needs to be taken into account for many non-linear processes as instantaneous currents may differ significantly from the average. Hence, a dynamic model including the temporal variation of the electron currents which goes beyond a simple bunching with twice the laser frequency but otherwise constant current is needed. Here we present a new time-dependent model to describe the laser generated currents and obtain simple expressions for the temporal evolution and resulting corrections of averages. To exemplify the model and its predictive capabilities we show the impact of temporal evolution, spectral distribution and spatial modulations on Ohmic heating of the bulk target material.

INTRODUCTION

The generation of energetig and dense electron currents by ultra-intense laser irradiation of solids has important impact on the heating of the solids [1], generation of resistive fields [2–4] development of current instabilities [5–7] and eventually the acceleration of ions at the plasma rear surface [8]. Its exact time-dependent calculation is of high relevance, e.g. due to non-linearities in the respective equations. Since there exists no simple complete and self-consistent explicit theory for the current generation from ultra-intense laser interaction with solids [9] and the relativistic dynamics is quite complex [10], one often conveniently falls back to the application of general conservation laws. It is very common to calculate the laser generated current of high energy electrons $j_h(t) = n_h(t)v_h(t)$ employing the energy flux density conservation equation [4, 11] assuming constant quantities (e.g. $\gamma_h(t) \approx \langle\gamma_h(t)\rangle$)

$$\chi\frac{a_0^2}{2} = \left(\langle\gamma_h(t)\rangle - 1\right)\langle n_h(t)\rangle\langle v_h(t)\rangle\,. \tag{1}$$

Here, $\langle ...\rangle$ denotes the time average over a laser period, $\chi a_0^2/2$ is the average energy flux density absorbed into energetic electrons (which may be differing significantly from total laser absorption) and $\gamma_h(t)$, $n_h(t)$, $v_h(t)$ are the time dependent energy, density and velocity in laser direction of laser accelerated electrons. Here and in the following we use dimensionless units, $c = m_e = n_c = \omega_0 = 1$. Assuming ad hoc an expression for the average electron energy [4, 11], $\bar\gamma_h = \sqrt{\chi/2}\,a_0 + 1$, and further assuming the temporal average Lorentz factor $\langle\gamma_h\rangle$ to be equal to the ensemble average $\bar\gamma_h$ and $\langle v_h\rangle \approx c$ as only relativistic intensities are discussed, $\gamma_h \gg 1$, Eqn. (1) can be readily solved for $\langle n_h\rangle = \langle\gamma_h\rangle\, n_c = \bar\gamma_h n_c$ and thus

$$\langle j_h\rangle \cong \bar\gamma_h n_c c \tag{2}$$

which coincides with heuristic arguments [5].Surprisingly, in literature the exact time-dependent form of Eqn. (1) is only rarely used. While (1) may still give good approximations for nanosecond or picosecond laser pulses we will demonstrate in this letter that they may fail for few-(ten-)femtosecond pulses. Generally, instantaneous values may differ significantly from the average values [12] which implies that generally the temporal evolution of $\gamma_h(t)$, $n_h(t)$ and $\beta_h(t)$ need to be considered and the averages be taken correctly,

$$\chi\frac{a_0^2}{2} = \langle\left(\gamma_h(t) - 1\right) n_h(t)v_h(t)\rangle\,. \tag{3}$$

For few-hundred femtosecond to few-picosecond laser pulses Eqn. (1) in fact turns out to be often useful due to *randomization* of trajectories of electrons during laser acceleration [13] or a laser period (which leads to apparent Maxwell-like integrated spectra), and averaging errors being small compared to typical shot-to-shot experimental uncertainties. Here we show that the situation can be different for ultra-short (up to few 10s of femtoseconds) high contrast laser pulses when significant electron phase randomization is not yet present.

PIC SIMULATIONS

We performed PIC simulations comparing to Eqn. 2. In order to keep the system as simple as possible we employ an artificial laser pulse with a short rise time of only $T/2$ followed by a flat top, spatially constant in the directions transverse to the propagation direction. The plasma slab was modeled by a 2 laser wavelengths thick flat preionized neutral ion-electron mixture with a density of $400n_c$ each, ion charge-to-mass ratio $e/2m_p$ (with proton mass m_p) and a small exponential preplasma with scale length $0.1\lambda_0$ added at the front. In the following

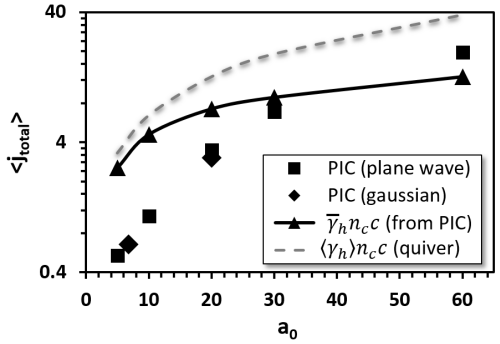

FIG. 1. Current density averaged over the simulation box in laser transverse direction and a 1λ long ROI covering the first two electron bunches inside the plasma. Squares (diamonds): PIC simulation employing plane (gaussian [1]) laser wave; triangles: $\bar{\gamma}_j$ from simulation (line is guide to the eye); dashed line: average quiver energy (5) (approx. ponderomotive).

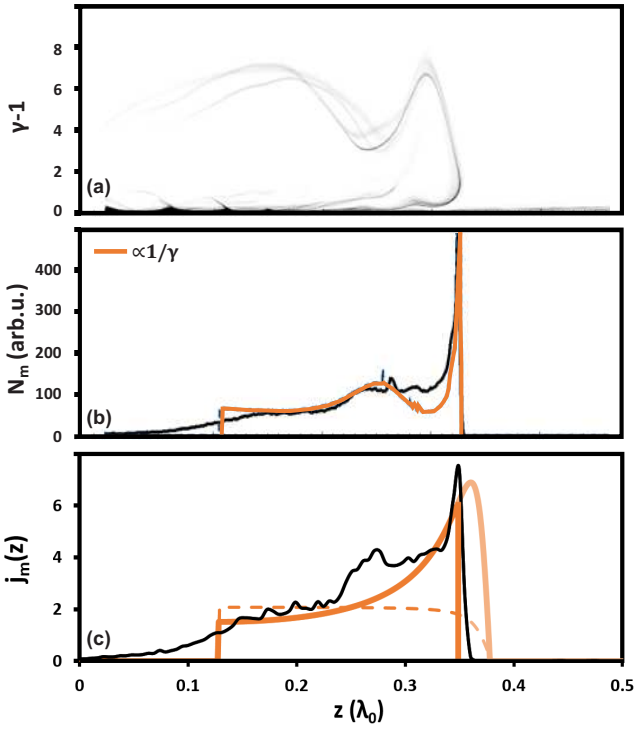

FIG. 2. Spatial (and assuming $v \approx c$ approximate temporal) evolution of energy (a), density (b) and current (c) of laser accelerated electrons. For (b) and (c) only electrons with $\gamma - 1 > m \equiv 1$ were considered. The figures average over the first 4 bunches. Orange lines are model predictions – (b): $n_e \propto 1/\gamma_h$ with γ_h from (a); (c): Eqn. (8) (solid) and corresponding expression for $f = const.$ (dashed), for $m = 0$ (light) and $m = 1$ (dark). $a_0 = 10$.

analysis we consider only those electrons originating from direct laser interaction, i.e. starting in the preplasma or skin-depth layer at the front. We average over a region of interest (ROI) comprising a distance of $1\lambda_0$ in laser direction starting $0.5\lambda_0$ inside the foil and extending over the full simulation box transverse direction. The time at which snapshots are taken corresponds to the time when after the laser pulse envelope is at maximum at the plasma front surface the first accelerated bunch reaches the rear of the ROI.

Fig. 1 shows the average current in laser direction of laser accelerated electrons inside the ROI compared to the analytical scaling Eq. (2) with $\bar{\gamma}_h$ extracted from the PIC simulation itself. It is readily seen that the popular scaling (2) does not describe the simulation results well, neither using $\bar{\gamma}_h$ nor $\langle\gamma_h\rangle$ (assuming transverse quiver motion as demonstrated in [14]). It overestimates the PIC results for $a_0 \leq 20$ while it significantly underestimates the currents for larger a_0. The differences are rather large with up to an order of magnitude for small a_0 or ultra-relativistic lasers $a_0 \gg 50$. It is important to note that since the current displayed in the figure comprises *all* laser accelerated electrons inside the ROI, it consists not only of electrons from two $2\omega_0$ bunches but due to dispersion also of slow moving electrons from earlier bunches. For this reason in the following we restrict our analysis to electrons with $\gamma_h - 1 > m$ with $m \equiv 1$. Yet, since the $2\omega_0$ bunches *inside* the ROI are also subject to dispersion and hence gradually leave the slow moving electrons behind, the dispersion is partially compensated and we may attribute a large part of the mismatch seen in Fig. 1 to Eqn. (2) not being valid in the simulation.

TIME AVERAGE AND TEMPORAL EVOLUTION OF LASER GENERATED ELECTRON CURRENT

In the following we model the current density for arbitrary $a_0 \ll \{n_e, m_i\}$ and including its temporal structure. Rewriting Eqn. (3) and the expression for $\langle j_h\rangle$ by replacing $n_h(t)$ with $n_h(t) \equiv \langle n_h\rangle f(t)$ introducing the normalized distribution function $f(t)$, and assuming that the electrons inside the plasma move ballisticly (i.e. mean free path $\gg$ foil thickness) in the direction of the laser, $v_z = \sqrt{\gamma^2-1}/\gamma_h$,

$$\chi\frac{a_0^2}{2} = \langle n_h\rangle \left\langle f(t)\,(\gamma_h(t)-1)\,\frac{\sqrt{\gamma_h(t)^2-1}}{\gamma_h}\right\rangle$$
$$j_h(t) = \langle n_h\rangle\, f(t)\frac{\sqrt{\gamma_h(t)^2-1}}{\gamma_h}, \qquad (4)$$

the unknown $\langle n_h\rangle$ can be eliminated. We are left with imposing a temporal density distribution of electrons $f(t)$ and energy evolution $\gamma_h(t)$.

In the following we discuss two cases, the mildly-relativistic and ultra-relativistic intensity case. For the mildly-relativistic case we will assume the electrons are

oscillating in the laser transverse electric field at the plasma front surface in a sufficiently thin layer, $p_{osc} = \hat{a}_0 \sin(\omega_0 t)$ (where $\hat{a}_0$ is the laser electric field strength at the plasma front surface, $\hat{a}_0 \approx 0.9 a_0$ in our simulations in agreement with [15]), and the longitudinal force exerted by the laser magnetic field component to be perfectly balanced by the plasma bulk response [16], i.e. $n_h \gg \langle \gamma_h \rangle$. The electron energy is then simply the quiver energy

$$\gamma_h(t) = \sqrt{1 + p_{osc}(t)^2}. \tag{5}$$

With $f(t) = const.$ this expression would reduce to $\bar{\gamma}_h = 2E\left(i\hat{a}_0\right)/\pi$ [17, 18] (where $E(x) = \int_0^{\pi/2} \sqrt{1 - x^2 \sin\phi}\, d\phi$ is the complete elliptical integral of the second kind) which approx. reproduces the Wilks ponderomotive scaling [18, 19]. However, following Fig. 2a,b, and as was established in [18], we will use

$$f(t) = f_0 \frac{1}{\gamma_h(t)} \tag{6}$$

in the following. This results in an average energy of laser accelerated electrons of $\bar{\gamma}_h = \left(\int_0^{\pi} \gamma_h(t)^{-1} dt\right)^{-1} = \langle {}^1\!/_{\gamma_h} \rangle^{-1}$. To give an explicit expression for f_0 we take the average $\langle f(t) \rangle = f_0 \langle {}^1\!/_{\gamma_h} \rangle \equiv 1$ and hence $f_0 = \bar{\gamma}_h = \frac{\pi}{2K(i\hat{a}_0)}$ where $K(x)$ is the complete elliptical integral of the first kind.

For the ultra-relativistic case we drop the restriction of electrons only oscillating transversely. Then γ_h reads [18]

$$\begin{aligned} \gamma_h(t) &= {}^{S(t)^2}\!/_2 + {}^3\!/_{S(t)^2} \\ S(t) &= \sqrt[3]{\sqrt{9 p_{osc}(t)^2 + 8} + 3 p_{osc}(t)}\,. \end{aligned} \tag{7}$$

Fig. 2c shows the temporal evolution of the current from the simulation with $a_0 = 10$ by plotting the current as a function of propagation distance into the plasma. Again we only consider energetic electrons with $\gamma - 1 > m \equiv 1$, hence $v > 0.86c$. Neglecting for now dispersion for the small distance traveled and assuming $v_z \approx c$, space and time are interchangeable and one can think of the figure as temporal evolution of the current of energetic laser generated electrons.
Clearly the current is not constant but shows the well-known pronounced $2\omega_0$ structure and an additional micro-structure. Calculating the model predictions from (4), the only free parameter remaining is χ which can be extracted from the simulation and for our conditions is always close to $0.1 - 0.15$. The result reads

$$j_h(t) = \frac{\chi a_0^2}{2} \frac{1}{\left\langle {}^{(\gamma_h - 1)\sqrt{\gamma_h^2 - 1}}\!/_{\gamma_h^2} \right\rangle} \frac{\sqrt{\gamma_h(t)^2 - 1}}{\gamma_h(t)^2} \tag{8}$$

for $0.5\mathrm{i} < t/2\pi < 0.5\mathrm{i} + 0.25$ where $\mathrm{i} \in \mathbb{N}$ and else $j_h(t) = 0$. This current is shown in Fig. 2c (orange line) and agrees well with the simulation result. For the mildly relativistic case the right hand side of (8) can be simplified by approximating the second term with $(3/\hat{a}_0)^{\sqrt{2}} + 1$. In complete analogy the temporal current evolution can be calculated for $f = const.$ (orange dashed line) as usually assumed in literature. However, in this case the predicted temporal evolution within a bunch would be inverse, increasing towards the end of the bunch, which contradicts the simulation result.

Given the simplicity of the model and approximations we made, the agreement of the model asuming $f \propto 1/\gamma_h$ with the PIC simulation is remarkable. Two distinct excursions from the prediction are seen in the figure and are due to a micro bunching effect of the bunch interacting with the bulk, which is not included in our model [14]. Another discrepancy is that the current does not immediately drop to zero after half a laser period but leaks into the theoretically empty region. We speculate this to be due to non-vanishing initial electron momenta or surface fields that cause a deviation from the plane transverse electromagnetic wave model assumption.

We can also calculate time averaged currents performing the time average of (4). We readily obtain for the case of moderate laser intensities, Eqn. (8), the result

$$\langle j_h \rangle = \chi \frac{a_0^2}{2} \left(\frac{\tan^{-1}\left(\hat{a}_0\right) \sqrt{\hat{a}_0^2 + 1}}{\tanh^{-1}\left({}^{\hat{a}_0}\!/_{\sqrt{\hat{a}_0^2 + 1}}\right)} - 1 \right)^{-1} \tag{9}$$

while for the ultra-relativistic case no analytic solution exists but Eqn. (4) must be solved numerically. Again, in order to compare to the PIC simulations, we compute the current taking only into account the electrons with kinetic energy larger than m, $\langle j_h \rangle_m$. Fig. 3 shows the PIC results together with the numerically obtained theoretical values. A very good agreement is achieved, considering the transition between the mildly relativistic and ultra-relativistic laser intensity regimes (dashed line). In contrast, using Eqn. (1), i.e. neglecting the temporal structure of n_h, γ_h and v_h, we would have significantly underestimated the current. (blue line).

DISCUSSION

The laser generated energetic electron current influences important physical mechanisms for which the time-dependence of the current has significant impact not only due to the modified expression for the average current but also due to the fact that generally current and time enter the models with different non-linearity. We want to demonstrate this by computing the resistive heating of the plasma bulk which is dominated by Ohmic heating over drag heating and diffusive heating [21]. The change of bulk electron temperature T_e over time is given by

$$\frac{3}{2} n_e T_e^{3/2} \frac{\delta T_e}{\delta t} = Z \Lambda j_h(t)^2 \tag{10}$$

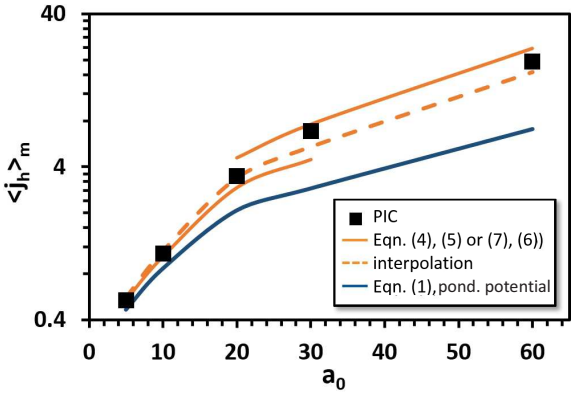

FIG. 3. Average current $\langle j_h \rangle|_m$ with $m = 1$ of energetic electrons in laser direction inside the ROI. Squares: PIC simulations; solid lines: model including time dependence for mildly relativistic ($a_0 < 25$) and ultra relativistic case ($a_0 > 25$); dashed line: empiric interpolation, weighting the ultra-relativistic case proportional to the approximate electron excursion length $\sqrt{\gamma_h/n_e}$ [20] relative to half a laser wavelength; solid blue line: neglecting time dependence. Laser absorption was extracted from the respective PIC simulation.

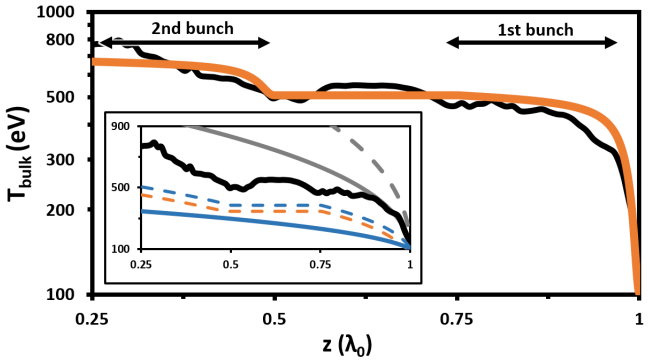

FIG. 4. Bulk temperature for PIC simulation $a_0 = 10$ from PIC simulation (black line) and model results from Ohmic heating equation with electron current (8) [23] (orange line). Inset: Comparison with other current models – orange dashed: as solid orange but taking $j_h = const$ during $2\omega_0$ bunches; blue solid (dashed): constant ($2\omega_0$ modulated) current from (1) and ponderomotive scaling; gray: $j_h = \bar{\gamma}_h n_c = const.$ with $\bar{\gamma}_h = \frac{\pi}{2K(i\hat{a}_0)}$ following (6) (in agreement with average energy from simuation) (solid) and ponderomotive scaling (dashed).

with charge state Z and Coulomb logarithm Λ and assuming the bulk current $j_b(t)$ to balance the laser generated electron current $j_h(t)$ [21, 22], which will be the case for approximately the magnetic diffusion time [3]. This equation was solved in [4] for constant j_h. As in the present condition of our PIC simulations j_h is not constant we have to apply (8). The calculated bulk temperature [23] (solid orange line) compares exceptionally well with the PIC simulation and especially is a much better model than that of the commonly assumed constant current (solid blue line).

From Fig. 4 we can conclude that a precise determination of the average laser generated electron current is important , which as shown above requires to take into account the spectral and temporal shape of the bunch (i.e. using (4) instead of (1), cp. dashed orange and blue lines). However, for ohmic heating, due to $j_h(t)$ entering non-linearly in Eqn. (10), the difference between either taking the thus calculated average current (9) together with simply assuming a $2\omega_0$ bunching with constant current within a bunch (dashed orange line) or taking the correct temporal evolution within a bunch, Eqn. (8) (solid orange line), is minor.

CONCLUSION

We have demonstrated that the calculation of the laser generated electron current is much more complex than using the simple equation $j_h = \langle \gamma_h \rangle n_c$. First, the kinematic, non-thermal spectral distribution has to be taken into account when calculating the average current density using the energy flux conservation. In our calculations the laser absorption taken from simulations is the only input parameter and we derived an expression for the average laser generated current. To derive the temporal evolution one simply has to take into account the $2\omega_0$ structure imprinted on the current, i.e. the bunch duration and spacing of a quarter laser period. Moreover, the temporal structure within a bunch is of importance. Additionally to our model, effects such as dispersion, front surface fields and interaction with bulk plasma oscillations inside the plasma slab can change the spectrum as well as temporal structure. These considerations are of general importance in all situations where the electron current or time enter a model non-linearly. Hence, we expect for example in the case of resistive heating and field generation [2–4] and therefore material dependent electron propagation [4–6] a significant improvement applying time-dependent models for the current evolution.

It is important to point out that model assumptions and PIC simulation parameters of a plane laser wave interacting with a planar cold target were deliberately chosen as illustrative and easy to study examples of the implications of Eqn. (4). In a real experiment the finite laser focal size, longer pulse duration and finite foil thickness will lead to a more complex situation, i.e. $\gamma_h(t)$ may become a complicated multi-parametric function and $f(t)$ may not follow the simple relation given above as e.g. target heating [24], instabilities [10, 25], density steepening [26] and refluxing electrons reflected from the target surfaces [27, 28] have to be taken into account. Additionally, in those cases the accelerated electrons eventually may show phase mixing so that $\gamma_h(t)$ differs and becomes randomized among the electrons.

The work has been partially supported by EC FP7 LASERLAB-EUROPE/CHARPAC (contract 284464) and by the German Federal Ministry of Education and Research (BMBF) under contract number 03Z1O511.

* t.kluge@hzdr.de; http://hzdr.de/crp

[1] Y. Sentoku, A. J. Kemp, R. Presura, M. S. Bakeman, and T. E. Cowan, Phys. Plasmas **14**, 122701 (2007); J. S. Green, K. L. Lancaster, K. U. Akli, *et al.*, Nat. Phys. **3**, 853 (2007); H. Nishimura, R. Mishra, S. Ohshima, *et al.*, Phys. Plasmas **18**, 022702 (2011); L. G. Huang, M. Bussmann, T. Kluge, *et al.*, Phys. Plasmas **20**, 093109 (2013).

[2] A. Bell, J. Davies, and S. M. Guerin, Phys. Rev. E **58**, 2471 (1998); E. D'Humières, J. Rassuchine, S. Baton, *et al.*, Eur. Phys. J.-S. T. **175**, 89 (2009); P. Norreys, D. Batani, S. Baton, *et al.*, Nucl. Fusion **54**, 054004 (2014); Y. Sentoku, E. D'Humieres, L. Romagnani, P. Audebert, and J. Fuchs, Phys. Rev. Lett. **107**, 135005 (2011); S. Chawla, M. S. Wei, R. Mishra, *et al.*, Phys. Rev. Lett. **110**, 025001 (2013).

[3] J. Davies, A. Bell, M. Haines, and S. Guérin, Phys. Rev. E **56**, 7193 (1997).

[4] P. Leblanc and Y. Sentoku, Phys. Rev. E **89**, 023109 (2014).

[5] J. Fuchs, T. Cowan, P. Audebert, *et al.*, Phys. Rev. Lett. **91**, 255002 (2003).

[6] M. Manclossi, J. J. Santos, D. Batani, *et al.*, Phys. Rev. Lett. **96**, 125002 (2006).

[7] F. Califano, T. Cecchi, and C. Chiuderi, Phys. Plasmas **9**, 451 (2002); M. S. Wei, F. N. Beg, E. L. Clark, *et al.*, Phys. Rev. E - Stat. Nonlinear, Soft Matter Phys. **70**, 1 (2004); K. Quinn, L. Romagnani, B. Ramakrishna, *et al.*, Phys. Rev. Lett. **108**, 135001 (2012).

[8] S. P. Hatchett, C. G. Brown, T. E. Cowan, *et al.*, Phys. Plasmas **7**, 2076 (2000); R. A. Snavely, M. H. Key, S. P. Hatchett, *et al.*, Phys. Rev. Lett. **85**, 2945 (2000); P. Mora, Phys. Rev. E **72**, 56401 (2005); J. Schreiber, F. Bell, F. Grüner, *et al.*, Phys. Rev. Lett. **97**, 45005 (2006); K. Zeil, J. Metzkes, T. Kluge, *et al.*, Nat. Commun. **3**, 874 (2012).

[9] A. Debayle, J. Sanz, L. Gremillet, and K. Mima, Phys. Plasmas **20** (2013), 10.1063/1.4807335.

[10] T. Kluge, J. Metzkes, K. Zeil, *et al.*, Phys. Plasmas **22**, 064502 (2015).

[11] M. G. Haines, M. S. Wei, F. N. Beg, and R. B. Stephens, Phys. Rev. Lett. **102**, 45008 (2009).

[12] H. Popescu, S. D. Baton, F. Amiranoff, *et al.*, Phys. Plasmas **12**, 63106 (2005).

[13] B. Bezzerides, S. J. Gitomer, and D. W. Forslund, Phys. Rev. Lett. **44**, 651 (1980).

[14] T. Kluge, M. Bussmann, T. E. Cowan, and U. Schramm, Nucl. Instruments Methods Phys. Res. A Spec. Issue Proc. Eur. Adv. Accel. Conf. 2015 *(submitted)*.

[15] A. Bourdier, Phys. Fluids **26**, 1804 (1983); C. Rödel, D. an der Brügge, J. Bierbach, *et al.*, Phys. Rev. Lett. **109**, 125002 (2012).

[16] M. Kaluza, *Characterisation of laser-accelerated proton beams*, Ph.D. thesis, TU München (2004).

[17] W. Yu, V. Bychenkov, Y. Sentoku, *et al.*, Phys. Rev. Lett. **85**, 570 (2000).

[18] T. Kluge, T. Cowan, A. Debus, *et al.*, Phys. Rev. Lett. **107**, 205003 (2011).

[19] S. C. Wilks, A. B. Langdon, T. E. Cowan, *et al.*, Phys. Plasmas **8**, 542 (2001).

[20] B. Chrisman, Y. Sentoku, and a. J. Kemp, Phys. Plasmas **15**, 056309 (2008).

[21] M. E. Glinsky, Phys. Plasmas **2**, 2796 (1995).

[22] A. R. Bell, J. R. Davies, S. Guerin, and H. Ruhl, Plasma Phys. Control. Fusion **39**, 653 (1997).

[23] We have to take into account a filamentary spatial modulation of the current in transverse direction, from the PIC simulation we infer an electron current density peak (along a filament) $F = 1.7$ times the average value. Extracting $j_h(t)$ from the simulation with $a_0 = 10$, we can solve the Ohmic heating equation and in deed find almost perfect agreement with the simulation when including the filamentation.

[24] L. G. Huang, M. Bussmann, T. Kluge, *et al.*, Phys. Plasmas **20**, 093109 (2013).

[25] Y. Sentoku, K. Mima, S.-i. Kojima, and H. Ruhl, Phys. Plasmas **7**, 689 (2000).

[26] A. Kemp, Y. Sentoku, and M. Tabak, Phys. Rev. Lett. **101**, 075004 (2008).

[27] A. J. Mackinnon, Y. Sentoku, P. K. Patel, *et al.*, Phys. Rev. Lett. (2002); R. Mishra, Y. Sentoku, and A. J. Kemp, Phys. Plasmas **16**, 112704 (2009).

[28] T. Kluge, W. Enghardt, S. D. Kraft, *et al.*, Phys. Plasmas **17**, 123103 (2010).